RESEARCH ARTICLE

CXCL2 attenuates osteoblast differentiation by inhibiting the ERK1/2 signaling pathway

Yang Yang, Xinying Zhou, Yuejun Li, Ajuan Chen, Wenquan Liang, Guojun Liang, Bin Huang, Qingchu Li* and Dadi Jin*

ABSTRACT

The C-X-C motif chemokine ligand 2 (CXCL2), a member of the CXC receptor ligand family, is involved in various immune and inflammatory processes, but its effect(s) on bone formation have not yet been reported. We report here that CXCL2 is enriched in bone marrow and show abundant expression of CXCL2 in osteoblasts of osteoporotic mice. CXCL2 neutralization within the bone marrow by using antibody alleviated bone loss in mice, indicating a negative role of CXCL2 in bone formation. In line with this, CXCL2 overexpression attenuated proliferation, as well as differentiation, of osteoblasts *in vitro*. By contrast, CXCL2 downregulation promoted osteoblast expansion and differentiation. Mechanistically, CXCL2 inhibits the ERK1/2 (MAPK3/1) signaling pathway in osteoblasts. Activation of ERK1/2 abolishes the inhibitory effect of CXCL2 in osteoblasts, whereas inactivation of ERK1/2 reverses the osteogenic role of CXCL2 inhibition. These results show that CXCL2 attenuates osteoblast differentiation through inhibition of the ERK1/2 signaling pathway. We demonstrate here that CXCL2 is a negative regulator of bone formation and clarify the responsible mechanisms. Therefore, pharmaceutical coordination of CXCL2 and of the pathways through which it is regulated in osteoblasts might be beneficial regarding bone formation.

KEY WORDS: Osteoblast, CXCL2, Osteoporosis, Bone formation, Differentiation, ERK1/2

INTRODUCTION

Osteoporosis is one of the most common diseases of bone metabolism and is characterized by decreased density of mineralized bone. It leads to induced mechanical strength and increased susceptibility to fractures, pain and disability (Glaser and Kaplan, 1997; Marini et al., 2016; National Clinical Guideline, 2012; Kanis et al., 2001). As the population is aging globally, incidence rates of osteoporosis and secondary fractures are rising rapidly (Lizneva et al., 2018; Abrahamsen et al., 2018; Ha, 2016; McNamara, 2010). The cellular pathology of osteoporosis mainly includes reduced activity of osteoblasts and increased activity of osteoclasts. The imbalance between bone formation and resorption leads to loss of bone mass (Manolagas, 2000). Moreover, the relationship between immune system and bone has long been speculated, as bone loss is a common condition in autoimmune and inflammatory disorders (Arron and Choi, 2000; D'Amelio et al., 2008).

During osteogenesis imperfecta (brittle bone disease), various factors participate in the process of the disease through complex biochemical reactions and cellular communication (Long, 2012). Runt-related transcription factor 2 (RUNX2) is an osteogenesis-related transcription factor, playing an important role in promoting the differentiation of bone marrow stem cells (BMSCs) into preosteoblasts and mature osteoblasts (Cargnello and Roux, 2011). Previous research has indicated that the mitogen-activated protein kinase (MAPK) signaling pathway plays crucial functions in regulating cellular physiology and pathology processes, such as cell expansion, differentiation, stress response and immune reactions (Cargnello and Roux, 2011; Boutros et al., 2008; Liu et al., 2007). Some studies have also shown that activation of the MAPK family members ERK1 and ERK2 (ERK1/2, officially known as MAPK3 and MAPK1, respectively) promotes expression of the downstream transcription factor RUNX2 (Greenblatt et al., 2013; Franceschi et al., 2007), which is expressed during differentiation of osteoblasts (i.e. osteogenic differentiation).

The chemokine ligand C-X-C motif chemokine ligand 2 (CXCL2), also known as macrophage inflammation protein 2 alpha (MIP-2a), affects neutrophil recruitment and activation through MAPK signaling by binding and activating its specific receptors, CXCR1 and CXCR2 (Wolpe et al., 1989; Rittner et al., 2007). By activating these receptors, the level of phosphorylation of the downstream CXCR pathway members ERK1/2, is increased (Scala, 2015). CXCL2 is synthesized in several of cell types, including macrophages and monocytes, and acts as a mediator of inflammation (Rittner et al., 2007). In the human body, the highest levels of CXCL2 are found in liver and bone (Fagerberg et al., 2014). Studies have revealed that CXCL2 promotes the development of osteoclasts (osteoclastogenesis) (Ha et al., 2010; Valerio et al., 2015) but whether CXCL2 influences other cell types in the bone is unknown. Since ERK1/2 signaling is downstream of CXCRs (Ha et al., 2010) and osteogenesis regulators, such as fibroblast growth factor (FGF; Cargnello and Roux, 2011), it is reasonable to investigate whether a correlation exists between osteoblastogenesis and CXCL2 through the ERK1/2 pathway.

In this study, we first identified high CXCL2 levels in human osteoporotic bone tissues. CXCL2 was also enriched in bone marrow. We next found that osteoblastic CXCL2 was overexpressed in a mouse model of osteoporosis, and that the process of osteoporosis was alleviated when CXCL2-induced chemotaxis was neutralized in the bone in response to anti-CXCL2 antibody injection (see Materials and Methods). Further, the results of *in vitro* experiments identified effects of CXCL2 on regulation of proliferation and differentiation in preosteoblasts. Mechanistically, CXCL2 suppresses the phosphorylation of ERK1/2 and leads to inhibition of differentiation in preosteoblasts. Overall, our study indicates that

Department of Orthopedics, Academy of Orthopedics Guangdong Province, the Third Affiliated Hospital of Southern Medical University, 510000 Guangzhou, China.

*Authors for correspondence (nyorthop@163.com; lqc16@263.net)

Y.Y., 0000-0003-2055-5778; X.Z., 0000-0002-0491-0170; Y.L., 0000-0002-4346-7458; A.C., 0000-0001-6391-9207; W.L., 0000-0003-0881-6808; G.L., 0000-0001-8620-8299; B.H., 0000-0001-6295-6647; Q.L., 0000-0002-5221-0195; D.J., 0000-0002-9448-2615

1

CXCL2 regulates bone formation via the ERK1/2 signaling pathway, and supports the finding that of CXCL2 being a novel target to stimulate osteogenesis in bone.

RESULTS

CXCL2 is increased in human osteoporotic bone

Previous studies have indicated that CXCL2 promotes osteoclastogenesis *in vitro* (Ha et al., 2010; Valerio et al., 2015). As bone resorption and osteoporosis are tightly coupled through bone metabolism, we analyzed whether a correlation exists between CXCL2 and osteoporosis. Analysis of CXCL2 levels in the human body required the use of clinical samples and to carry out ELISAs. To achieve this, we collected 42 blood samples from patients who underwent lumbar surgery in our department. Of these, 23 were samples of peripheral blood and 19 were samples of blood extracted from cancellous bone (also know as the trabeculae area in bone) of the lumbar vertebrae (hereafter referred to as cancellous blood). We also measured the clinical bone marrow density (BMD) of healthy individuals and osteoporosis patients for further analysis. Gender and age within each group were statistically not significant (Tables S1 and S2).

First, a comparison between CXCL2 concentrations in peripheral and cancellous blood was made. The result indicated that cancellous blood had a higher level of CXCL2 than peripheral blood (Fig. 1A). Results showed an enrichment tendency in bone marrow, which is in accord with results of earlier studies (Fagerberg et al., 2014; Trošt et al., 2010). Moreover, combined with clinical BMD data, the concentration of CXCL2 in bone marrow had a positive correlation with BMD (Fig. 1B), and cancellous blood of osteoporosis patients had significantly higher CXCL2 levels than blood of non-osteoporosis patients (Fig. 1C). However, the concentration of CXCL2 in peripheral blood had a correlated negatively with the BMD (Fig. 1D), and CXCL2 levels in the osteoporosis group were lower than in the control group (Fig. 1E). These findings suggest that human bone marrow contains higher levels of CXCL2 and that CXCL2 plays a role in osteoporosis.

Secretion of CXCL2 is increased in the bone of osteoporotic mice

The results described above suggest that CXCL2 is active in osteoporotic bone marrow, but the source of this chemokine is still unclear. The CXC family has previously been reported to target cell types other than immune-related cell lines (Strieter et al., 2007; Huang et al., 2016). Therefore, it seemed reasonable to investigate whether increased CXCL2 has an effect on osteogenesis.

We explored CXCL2 levels in osteoblasts derived from the bone marrow of osteoporotic mice. To create the osteoporosis mouse model, ovariectomy (OVX) was performed on female mice, resulting in mice suitable to study postmenopausal osteoporosis (hereafter referred to as postmenopausal OVX mice). To verify the validity of the model, we observed the appearance of uteri (Fig. 2A), photographed bone details by using micro-CT scanning (Fig. 2B) and compared the BMD results (Table 1) of OVX mice with those of female controls (untreated mice, aged for 8 weeks and undergoing a sham operation, then maintained 3 months). Then, we marked the mature osteoblastic biomarker osteocalcin (OCN) as well as CXCL2 by performing double-labeling immunofluorescence. Results showed that osteoblasts in the bone marrow of osteoporotic mice secreted CXCL2 at higher levels, and that the ratio of CXCL2-positive osteoblasts to the numbers of total osteoblasts in the area comprising trabeculae, within osteoporotic OVX mice was significantly higher than that in control mice (sham) (Fig. 2C). On this basis, we concluded that secretion of CXCL2 in osteoblasts of osteoporotic is increased and that CXCL2 might influence bone formation through its effect on osteoblasts.

Neutralization of CXCL2 in bone marrow of osteoporotic mice alleviates osteoporosis

The results above indicated that osteoblastic CXCL2 in bone marrow is related to osteoporosis. We, therefore, performed a 'reverse' experiment to identify the effect of neutralizing CXCL2 in osteoporotic bone marrow. For this, we used 1.2 year-old male mice (hereafter referred to as old mice) in addition to the postmenopausal OVX mice to simulate the osteoporotic bone marrow micro-environment *in vivo*. To inhibit CXCL2-induced chemotaxis of osteoblasts, CXCL2 neutralizing antibody (see Materials and Methods) was injected into the bone marrow cavity of femora. Antibody injection (AbI) was used for the experimental group and injection with normal, i.e. isotonic, saline solution (0.7% NaCl) was used as negative control. Western blotting for CXCL2 levels in the femora showed that the neutralization was effective (Fig. 3A).

Results of immunohistochemistry staining (IHC) depicted in Fig. 3B showed that OCN-positive cell numbers on the bone surface
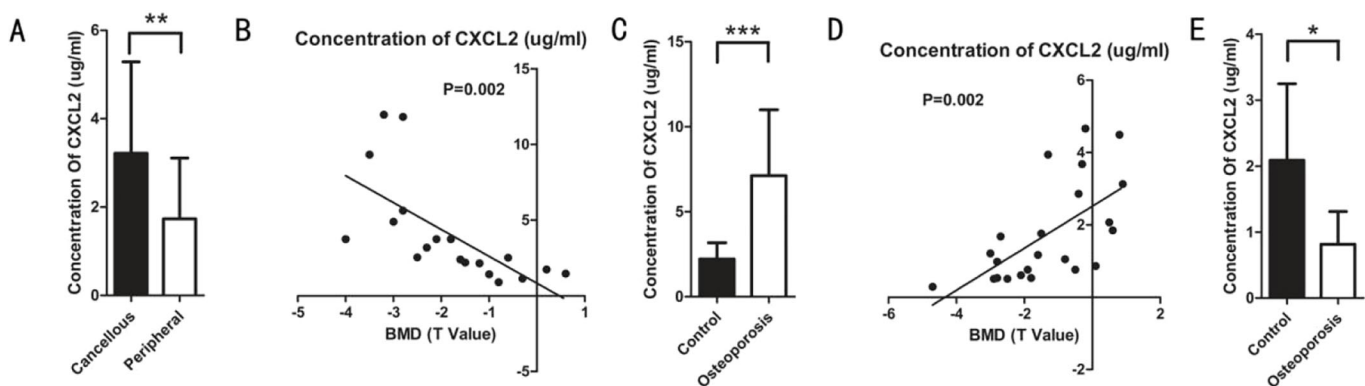
Fig. 1. Human bone marrow (peripheral blood) contains higher levels of CXCL2 than peripheral blood, and CXCL2 plays a role in the osteoporotic process. ELISA was used to detect OD values of clinical serum samples. BMD data were collected from bone densitometry examinations after hospitalization. (A) Comparison of CXCL2 concentrations in cancellous blood and peripheral blood. (B) Linear analysis of BMD and CXCL2 concentrations in cancellous blood, $n=19$. (C) Comparison of CXCL2 levels in blood from healthy humans (Control) and osteoporosis patients. $n=11$ for control and $n=8$ for osteoporosis. (D) Linear analysis of BMD and CXCL2 concentrations in peripheral blood, $n=23$. (E) Comparison of peripheral CXCL2 levels in blood from healthy humans (Control) and osteoporosis patients. $n=16$ for control and $n=7$ for osteoporosis. The data are the mean±s.d. *$P<0.05$; **$P<0.005$; ***$P<0.0005$.
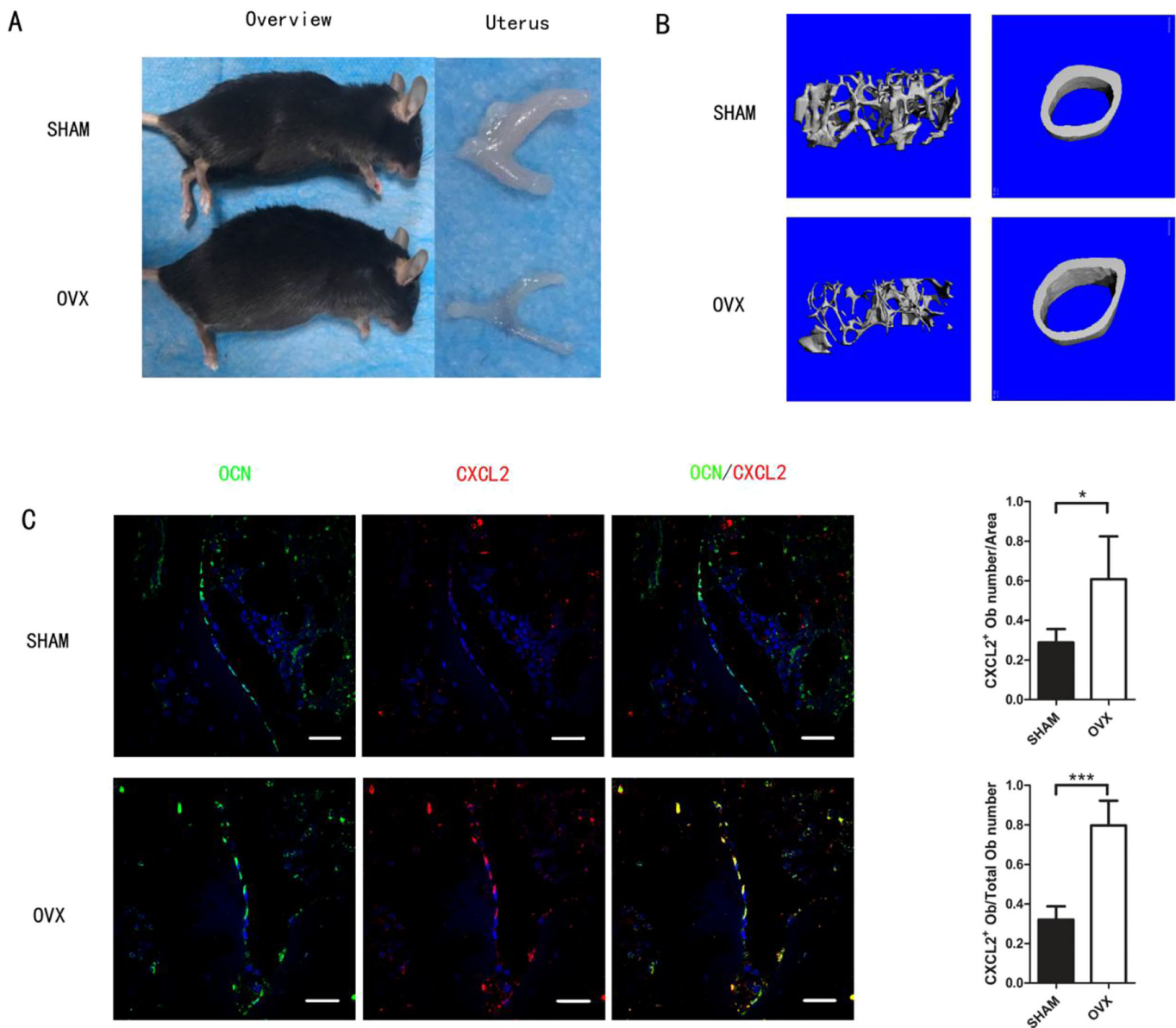
Fig. 2. The osteoporotic mouse model and increased levels of CXCL2 osteoblasts of osteoporotic mice. (A) Image of a sham-operated (SHAM) and OVX mouse (overview) and their respective uterus. (B) Micro-CT scanning and 3D reconstruction images of the bone details of sham-operated and OVX mice. (C) Representative photomicrographs of double-labelling immunofluorescence of CXCL2 (red) and osteocalcin (OCN, red) in bone marrow. Merged images (OCN+CXCL2) are shown on the right. The graphs show the ratio of CXCL2+Ob numbers versus the area of trabeculae (top) and the ratio of CXCL2$^+$ Ob numbers versus the total number of osteoblasts (Total Ob number) (bottom) in sham-operated and OVX mice. Scale bars: 20 μm. n=6 per group. *P<0.05, ***P<0.0001.

were significantly increased in the AbI group (Fig. 3B). The micro-CT scanning photos also confirmed that both the number and area of trabecula in the AbI group were conspicuously bigger compared with those in the negative control group (Fig. 3C). BMD analysis showed significant improvement of the cancellous bone, trabecula number, trabecula separation, cortical BMD and cortical trabecular bone volume fraction (BV/TV) (Fig. 3D) in the AbI-treated group. From this, we concluded that to reduce CXCL2 levels in bone marrow is an efficient way to alleviate osteoporosis in mice, and that CXCL2 might play an essential role in osteogenic regulation.

CXCL2 attenuates expansion of MC3T3-E1 cell

Our results confirmed the manifestation of CXCL2 in osteoporosis, and the reverse experiment also indicated that CXCL2 may regulate

the bone formation process *in vivo*. To further investigate this, we performed osteoblast-related functional experiments by regulating expression levels of CXCL2.

First, we investigated the effect of CXCL2 on the expansion of osteoblasts *in vitro*. MC3T3-E1 cells, the progenitors of osteoblasts, were transfected with siRNA and plasmid vectors to down- or up-regulate the expression levels of CXCL2. Effects of transfection were measured using quantitative PCR (qPCR) and CXCL2 mRNA expression was measured to verify the efficiency (Fig. 4A). Immunofluorescence staining of the proliferation marker protein Ki-67 showed that downregulation of CXCL2 causes MC3T3-E1 cells to proliferate faster than the control group, whereas upregulation of CXCL2 resulted in a decrease in proliferation of MC3T3-E1 cells (Fig. 4B). The CCK8 assay, used to assess cell

Table 1. Comparison of micro-CT scanning parameters of cancellous and cortical bone in sham-operated and OVX mice

	SHAM	OVX	OVX/ SHAM	P-value
Cancellous bone				
BMD [mg/cm³]	314.475±17.105	246.413±63.971	0.8	0.021
BV/TV	0.041±0.004	0.029±0.003	0.7	0.022
Tb.N [1/mm]	3.480±0.084	2.791±0.225	0.8	0.021
Tb.Sp [mm]	0.311±0.008	0.385±0.012	1.2	0.004
Tb.Th [mm]	0.061±0.007	0.044±0.004	0.7	0.012
Cortical bone				
BMD [mg/cm³]	811.825±18.370	668.375±84.271	0.8	0.001
BA [mm²]	0.883±0.06	0.669±0.059	0.8	0.018
TA [mm²]	1.993±0.132	1.947±0.083	1.0	0.686
BA/TA	0.436±0.016	0.358±0.017	0.8	0.003

n=10 per group. *$P<0.05$ was considered statistically significant. SHAM, sham-operated mice; OVX/SHAM, ratio of OVX mice to sham-treated mice; BMD, bone marrow density; BV/TV, trabecular bone volume fraction; Tb.N, trabecular number; Tb.Sp, separation of cancellous trabecula; Tb.Th, thickness of cancellous trabecula; BA, bone cross-sectional area; TA, total cross-sectional area; BA/TA, ratio of BA to TA

proliferation, also confirmed this result (Fig. 4C). We then performed flow cytometry analysis to determine whether CXCL2 has an effect on apoptosis in MC3T3-E1 cells. However, no significant difference was found (Fig. 4D) and, when compared with the data above, we concluded that CXCL2 attenuated MC3T3-E1 cell expansion by increasing proliferation.

CXCL2 suppresses differentiation of MC3T3-E1 cells

We further designed a series of experiments to evaluate the effect of CXCL2 on osteoblast differentiation. We chose the mature osteoblastic bio-marker osteocalcin (OCN) and the osteogenic-related transcription factor RUNX2 as targets to evaluate differentiation levels. Real-time PCR showed that mRNA expression of *Ocn* and *Runx2* in MC3T3-E1 cells is significantly increased, whereas that of *Cxcl2* was decreased; upregulation of *Cxcl2* expression had the opposite effect (Fig. 5A). We also confirmed similar trends in osteoblasts primary cultures (Fig. S1A). Western blotting analysis showed the same result at the protein level (Fig. 5B). Macroscopically, both staining with alkaline phosphatase (ALP) and Alizarin Red staining (ARS) suggested that overexpression of CXCL2 suppresses the differentiation of MC3TE-E1 cells but that its knockdown promotes the cell differentiation (Fig. 5C). These data indicate that CXCL2 suppresses the differentiation of MC3T3-E1 cells through a currently undefined mechanism.

CXCL2 inhibits ERK1/2 signaling upstream of RUNX2 in MC3T3-E1 cells

The functional *in vitro* experiments described above suggest that osteoblastic CXCL2 is crucial to regulate osteogenesis. Previous studies have indicated that the ERK1/2 signaling pathway may be a positive regulator of the osteogenic process (Cargnello and Roux, 2011; Murakami et al., 2017). Further, CXCL2 has been reported as an upstream regulator of ERK1/2 signaling (Ha et al., 2010). Therefore, we next tried to determine whether activation of the ERK1/2 signaling pathway has a role in CXCL2-dependent bone formation.

First, MC3T3-E1 cells were treated with siRNA targeting *Cxcl2* (siRNA CXCL2) or control siRNA (siRNA NC), or with plasmids overexpressing FLAG-tagged CXCL2 (pCMV-Flag-CXCL2) or not (pCMV-Flag-NC) and performed western blot analysis to detect the levels of phosphorylated ERK1/2 (pERK1/2). We found that

phosphorylation of ERK1/2 was induced when osteoblastic CXCL2 was knocked down using RNA interference (RNAi), whereas overexpression of CXCL2 inhibited phosphorylation of ERK1/2 (Fig. 6A). This result indicated that high activity of ERK1/2 signaling is required during differentiation. Then, MC3T3-E1 cells were transfected either with siRNA CXCL2 and treated the ERK1/2 inhibitor SCH772984 (Fig. 6B) or were transfected with pCMV-Flag-CXCL2 and treated with the ERK1/2 activator C6 ceramide (Fig. 6C). The results showed that SCH772984 reversed the effect siRNA CXCL2 has on RUNX2 and OCN expression, i.e. RUNX2 and OCN levels were reduced (Fig. 6B). C6 ceramide, however, increased RUNX2 and OCN levels in MC3T3-E1 cells transfected with pCMV-Flag-CXCL2 (Fig. 6C). Importantly, ALP staining and ARS showed that inhibition of ERK1/2 in response to SCH772984 suppressed the differentiation process of MC3T3-E1 cells (Fig. 6D), whereas activation of ERK1/2 in response to C6 ceramide increased cell differentiation (Fig. 6E). Together, our *in vitro* studies lend support for a central role of CXCL2 in the regulation of differentiation in pre-osteoblasts through ERK1/2 signaling.

DISCUSSION

In this article, we defined the essential status of CXCL2 in the regulation of osteoblastogenesis. We observed an increase in CXCL2 expression in osteoporotic osteoblasts *in vivo* and a reduction in osteoblastic differentiation when osteoblastic CXCL2 was overexpressed *in vitro*. By using a conditional CXCL2 knockdown and CXCL2 overexpression in cells, we further determined that CXCL2 prevents preosteoblast differentiation through inhibition of the ERK1/2 signaling pathway.

Traditionally, CXC-motif chemokines are widely expressed in a variety cell types to mediate multiple immune and inflammatory reactions (Rittner et al., 2007; Wong et al., 2016; Vandercappellen et al., 2008; Ansel and Cyster, 2001). Effector cells, such as mononuclear macrophages, granulocytes and lymphocytes, exhibit a feed-back response when CXC ligands (CXCLs) specifically bond with their membrane receptors (CXCRs) (Baggiolini, 1998; Rollins, 1997). This way, cellular physiology and pathology processes, such as cell growth (Van Sweringen et al., 2011), differentiation (Baird et al., 1999; Lasagni et al., 2007), apoptosis (Hu and Colletti, 2010), distribution (Lasagni et al., 2007), infection (Wasmuth et al., 2009), injury (Van Sweringen et al., 2011; Clarke et al., 2011), neoplasia (Ijichi et al., 2011) and tumor metastasis (Verbeke et al., 2011) are regulated. However, some studies have identified functions of the CXC family in other aspects, such as the regulation of angiogenesis and vascular remodeling (Strieter et al., 2007). A recent study by us revealed that CXC-motif chemokines can affect non-immune cells through protein interactions and cellular communication. CXCL9, for example, regulates angiogenesis and osteogenesis by binding to vascular endothelial growth factor (VEGF) (Huang et al., 2016). These findings indicated that the CXC family plays an essential role in adjusting physiology and pathology in different tissues and organs.

Activation of CXCL2 expression has been reported in several situations, such as stress (Maeda et al., 2015), malignancies, rejection diseases (Kageyama et al., 2018) and acute injuries (Qin et al., 2017). Liver and bone marrow are the two tissues in the human body with the highest CXCL2 levels (Fagerberg et al., 2014). During bone resorption, it has been confirmed that CXCL2 enhances osteoclastogenesis through ERK1/2 signaling (Ha et al., 2010). However, there are not many studies that focus on the relationship between CXCL2 and osteoblastogenesis. In one, Trošt et al. found differences of *Cxcl2* expression in cultured primary osteoblasts derived from osteoporotic and non-osteoporotic patients
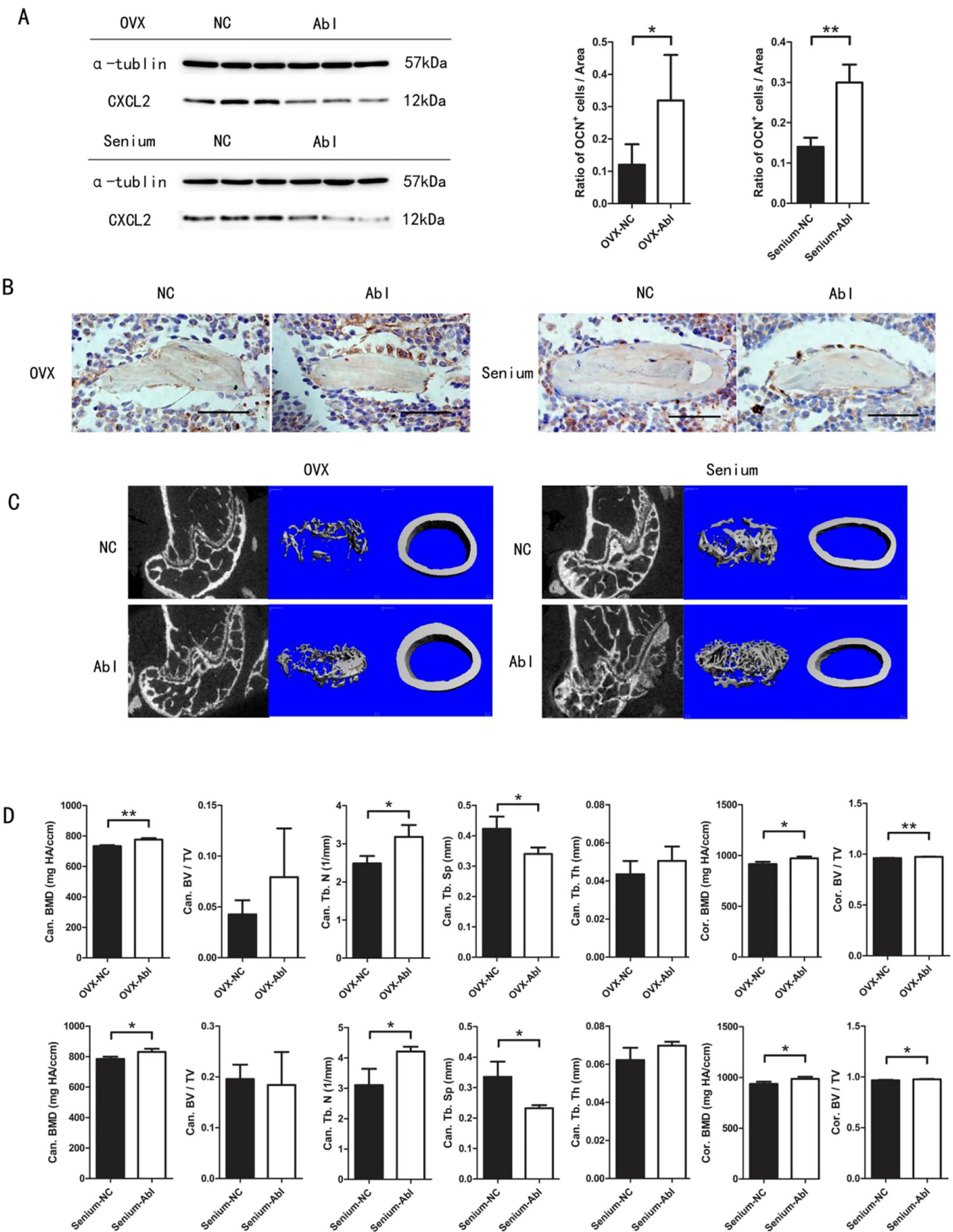
Fig. 3. See next page for legend.

Fig. 3. Neutralization of CXCL2 in bone marrow alleviates osteoporosis in mice. (A) Protein levels of CXCL2 in OVX (top blot) and old mice (Senium; bottom blot) that had been injected with saline as negative control (NC) or antibody (Ab I) were analyzed by western blotting. Protein levels of α-tubulin were used as control. Protein samples were extracted from mouse femora. (B) Immunohistochemistry images showing osteocalcin (OCN) in sections of trabecular bone in the distal femora of OVX and old mice injected with saline as NC or Ab I. The two bar graphs on the top right of the figure show the ratio of OCN-positive cell numbers and trabecula bone area. Scale bar: 50 µm. n=6 per group. (C) Micro-CT scanning and three-dimensional reconstruction images of distal and middle femora shafts from OVX and old mice treated as described in B. (D) Quantification of cancellous BMD (Can. BMD), cancellous BV/TV (Can. BV/TV), the number of cancellous trabecula (Can. Tb.N) and separation of cancellous trabecula (Can.Tb. Sp.), the thickness of cancellous trabecula (Can. Tb. Th), cortical BMD (Cor. BMD) and cortical BV/TV (Cor. BV/TV) in OVX and old mice injected with NC or Ab I. n=5 mice for each group. *P<0.05, **P<0.001.

(Trošt et al., 2010). Here, we provided evidence of increased CXCL2 protein levels in bone tissues of clinical osteoporosis patients. In addition, we created an osteoporosis mouse model to explore CXCL2 protein levels in osteoblasts. The results of our current study were positive and validated our previous study. Further, we proved the increase of CXCL2 to be a cause but not a result in this process, indicating that increased levels of CXCL2 protein within bone marrow may have subtle effects on the micro-environment of bone marrow leading to a result of less bone formation. The stabilization of the micro-environment is very important to the balance of bone remodeling.

Since ERK1/2 signaling is upstream of RUNX2 (Murakami et al., 2017) and RUNX2 regulates osteogenic differentiation in the formation of mature osteoblasts, we verified the correlation between CXCL2, RUNX2 expression and ERK1/2 activation. Surprisingly, phosphorylation of ERK1/2 was inhibited at high CXCL2 protein levels, which contradicts the results described by Ha et al. (2010). Our results indicate that CXCL2 does not suppress the differentiation of osteoblasts through binding to its receptor to activate downstream ERK1/2 signaling. Although it is reasonable to hypothesize that mediators exist that cooperate with CXCL2 in order to regulate bone formation via ERK1/2 signaling, the mechanisms still need to be explored. FGF/FGF receptor (FGFR) signaling, for example, is important in the regulation of bone formation (Ornitz and Marie, 2002), and is also upstream of ERK1/2 (Eswarakumar et al., 2005). FGF would be a potential mediator if its family members were to interact with CXCL2. It might be possible to identify gene functions or protein interactions within this biological process by comparing bone marrow samples from healthy individuals to those of osteoporosis patients by using high throughput sequencing techniques.

In summary, our study not only identified CXCL2 as a regulator of osteogenesis but also verified that CXCL2 can have effects on cellular physiology and pathology than are broader than conventionally understood. Although we failed to detect the protein interactions with CXCL2 that contribute to the regulation of bone formation, our data show that CXCL2 neutralization can alleviate osteoporosis in mice and revealed ERK1/2 signaling as being crucial in osteogenic regulation. Pharmaceutical therapies that target gene expression or protein levels of CXCL2, or signaling pathways such as those comprising ERK1/2 might be able to re-balance the micro-environment within bone marrow, thereby facilitating bone formation.

MATERIALS AND METHODS
Patient data and clinical samples
A total of 23 samples of peripheral blood and 19 samples of blood extracted from cancellous bone marrow of the lumbar vertebrae (cancellous blood) were collected in the Department of Spine Surgery, (the Third Affiliated Hospital of Southern Medical University, Guangzhou, China) between January 2018 and April 2019. Cancellous blood samples were extracted from patients who underwent lumbar surgery of pedicle screw placement. After tunnels of lumbar pedicles were drilled, the surgeon penetrated the vertebra to gather the cancellous blood. Blood samples were kept for 30 min, and then centrifuged at 4°C for 15 min, 1240 *g*. Serum samples were collected and then stored at −80°C. The BMD for every patients was recorded as the T-score, after dual-photon absorptiometry (DPA) after hospitalization. Osteoporosis was diagnosed at a T value of below −2.5. All patients were first diagnosed suffering from disc degeneration disease, none of the osteoporosis patients had received anti-osteoporosis treatment. Gender and age within groups were statistically not significant (Tables S1 and S2). The above process was signed as informed consent regarding all patients and permitted by the Ethics Committee of the hospital.

Enzyme-linked immunosorbent assay
To analyze CXCL2 levels in serum, enzyme-linked immunosorbent assays (ELISAs) were performed using the CXCL2 ELISA kit from Elab Science (E-EL-M0019c) following the manufacturer's instructions. The OD_{450} values were measured with an ultraviolet spectrophotometer (NanoVue Plus, GE Healthcare).

Mice
C57BL/6 background mice were purchased from The Experimental Animal Center of Southern Medical University (Guangzhou, China). Import, transport, housing and breeding of all mice was carried out according to the recommendations from the Southern Medical University (Guangzhou, China) 'The use of non-human primates in research.' To prevent suffering, mice were killed by cervical dislocation. All procedures involving mice were approved by the Southern Medical University Animal Care and Use Committee.

Establishment of the osteoporosis mouse model
Female mice underwent ovariectomy at the age of 8 weeks and were maintained for three months to create the estrogen-related (postmenopausal) osteoporosis OVX mouse model; mice in the control group underwent sham operation. Each group contained ten mice. Femora were dissected while the osteoporosis mouse model was established. In the reverse experiment, old (1.2 years) males were additional purchased and used as the aging-related osteoporosis model. The weight and physique of mice were approximately the same. To compare the osteoporotic bone marrow micro-environment *in vivo*, we used 1.2-year-old male mice (old mice).

In vivo neutralization of CXCL2 in bone marrow
We performed medullary cavity injection to neutralize CXCL2 in the bone marrow of OVX and old mice. CXCL2 neutralizing antibody (R&D, AF-452-NA, neutralizing CXCL2-induced chemotaxis) was injected at a concentration of 1 µg µl⁻¹ per 5 µl into the medullary cavity of femora through a hole burrowed into the joint surface of distal femora using an electric drill and a microinjector. This surgery was done at the same time as the ovariectomy to obtain OVX mice. Control mice (five mice per group) were injected with 5 µl normal saline solution (0.7% NaCl). Mice were continuously bred for 3 months and underwent intraperitoneal injection with 200 µl CXCL2 neutralizing antibody at a concentration of 0.025 µg µl⁻¹ twice per week. Femora were dissected 3 months after surgery.

Micro-CT analysis
Mouse femora were fixed for 48 h in 4% paraformaldehyde and analyzed at 10 µm resolution on a micro-CT scanner (Viva CT40; Scanco Medical AG, Bassersdorf, Switzerland). In brief, the lower growth plate within each femur was scanned cross-sectionally and moved for a total of 300 slices. Morphometric analysis was performed by using the first slice, in which the femoral condyles were totally merged and the progress was extended proximally for 100 slices. We manually segmented the cancellous bone from the cortical shell on the ten key slices and morphed the contours to all of the slices automatically. We also performed micro-CT imaging of the diaphysis shaft of the femur and evaluated 100 slices. The 3D structures
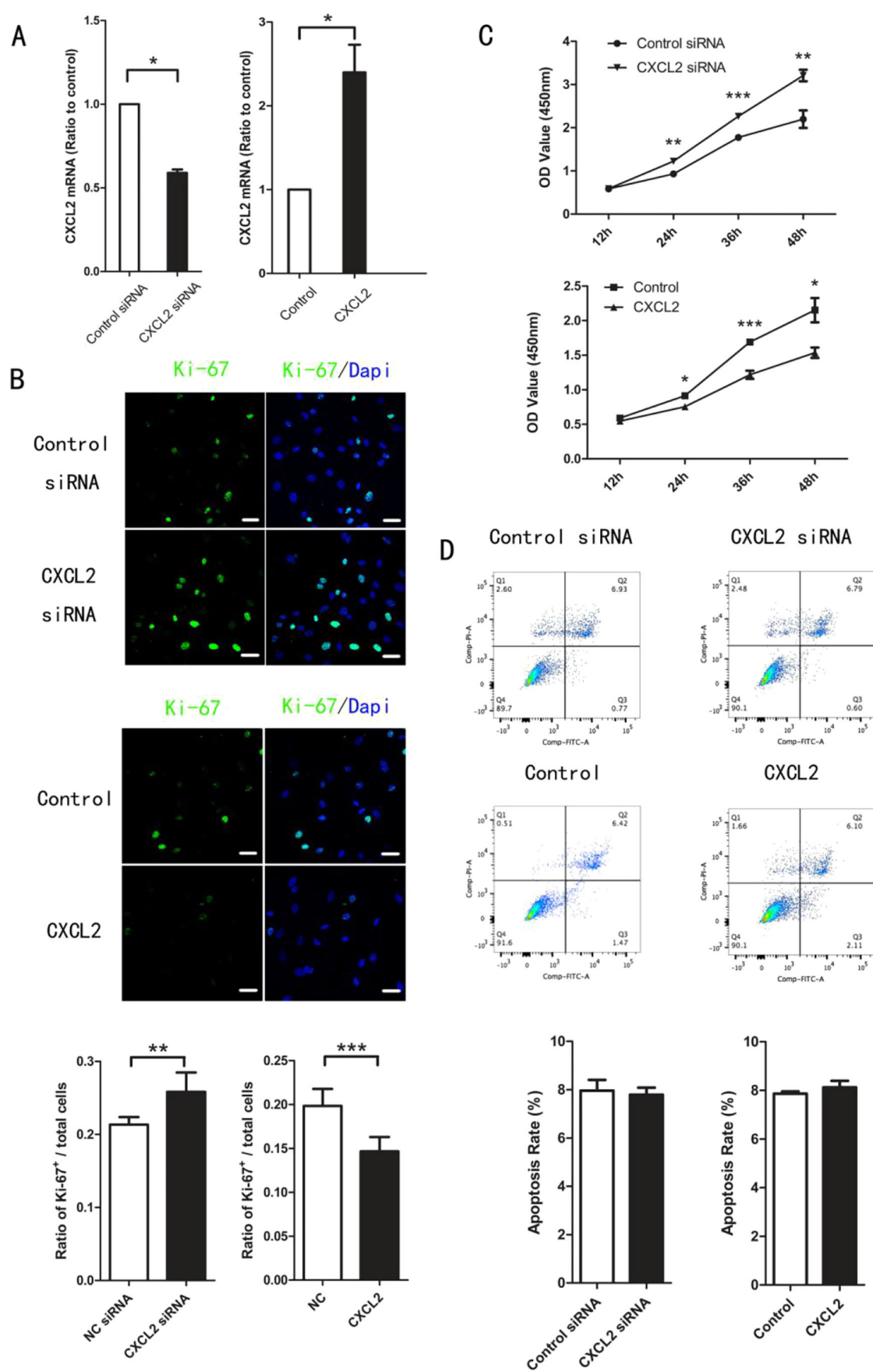
Fig. 4. See next page for legend.

Fig. 4. CXCL2 attenuates expansion of MC3T3-E1 cell *in vitro*. (A) Left: *Cxcl2* mRNA expression in MC3T3-E1 cells transfected with negative control siRNA or with siRNA targeting *Cxcl2*. Right: MC3T3-E1 cells stably expressing the negative control vector pCMV-Flag-NC (Control) or FLAG-tagged CXCL2 (pCMV-Flag-CXCL2 (CXCL2). *n*=6 per group. (B) Immunofluorescence images of MC3-T3-E1 cells transfected with negative control siRNA (control siRNA), siRNA targeting Cxcl2 (CXCL2 siRNA), pCMV-Flag-NC (Control) or pCMV-Flag-CXCL2 (CXCL2) (top); scale bars: 10 µm. Bar graphs showing the ratio of Ki-67-positive cells to the number of total cells. *n*=6 per group. (C) Transfected MC3-T3-E1 cells were seeded in 96-well plates and cell proliferation was assayed by CCK8 assay at the indicated days. (D) Transfected MC3-T3-E1 cells were analyzed by flow cytometry to measure apoptosis (top). Bar graphs comparing the rate of apoptosis each group (bottom); no significant differences were detected. *n*=6 per group. *$P<0.05$, **$P<0.001$, ***$P<0.0001$.

of trabecular and cortical bones were constructed, and the ratio of trabecular bone volume to total local volume (BV/TV), trabecular thickness (Tb. Th), trabecular number (Tb. N), trabecular separation (Tb. Sp) cortical bone area (BA) and total area (TA) were analyzed.

Immunostaining of femur slices and histomorphometric analysis
Mouse hindlimb tissues were fixed for 48 h in 4% paraformaldehyde and then decalcified in 15% ethylenediaminetetraacetic acid (EDTA pH 7.4) at 4°C for 21 days. Tissues were then embedded in paraffin and sagittal oriented sections of 2–5 mm were prepared for histological analysis. Incubation with primary antibody against mouse osteocalcin (Abcam, #Ab93876, 1:200) was overnight at 4°C for immunohistochemistry. Primary antibodies specific to mouse osteocalcin (Santa Cruz, SC365797,

1:200) and mouse CXCL2 (R&D, AF-452-NA, 1:100) were used for double-labeling immunofluorescence staining. Immunohistochemistry sections were observed and photographed using an Olympus BX51 microscope; double-labeling immunofluorescence sections were photographed using a laser scanning confocal microscope (FV1200 Olympus, Japan). Immunostaining was evaluated by calculating the ratio of CXCL2-positive cells to total osteoblasts within the trabecula area. At least six different images at 60× magnification for double-labeling immunofluorescence and 40× magnification for immunohistochemistry were taken, and evaluated using ImageJ. All mice in the experiment were examined. Three equidistant sections spaced 200 µm apart throughout the mid-sagittal section of femora were analyzed.

Cell culture and transfection
The MC3T3-E1 osteoblast progenitor cell line was purchased from the Cell Bank of Chinese Science Academy, Shanghai (GNM15), and was prepared for the following *in vitro* experiments. Cells were cultured in α-MEM with nucleosides (Gibco) supplemented with 10% fetal bovine serum (Gibco), at 37°C under 5% CO_2. To induce osteogenic differentiation (Huang et al., 2015, 2016), inducing medium, i.e. complete α-MEM, substituted with 100 µg ml^{-1} ascorbic acid (Sigma-Aldrich) and 10 mM β-glycerol phosphate (Sigma-Aldrich) was added to confluent cells. To transfect MC3T3-E1 cells, Lipofectamine 3000 (Invitrogen) was used following the manufacturer's instructions of transfection kit (Invitrogen) and siRNA CXCL2 in Opti-MEM (Gibco) was used to knock down expression of CXCL2. Cells in the control group were treated with negative control siRNA (random sequence). To overexpress CXCL2, cells were transfected with pCMV plasmid vector expressing-FLAG-tagged CXCL2 (pCMV-Flag-CXCL2) following the manufacturer's instructions (Invitrogen). Cells in the control group were
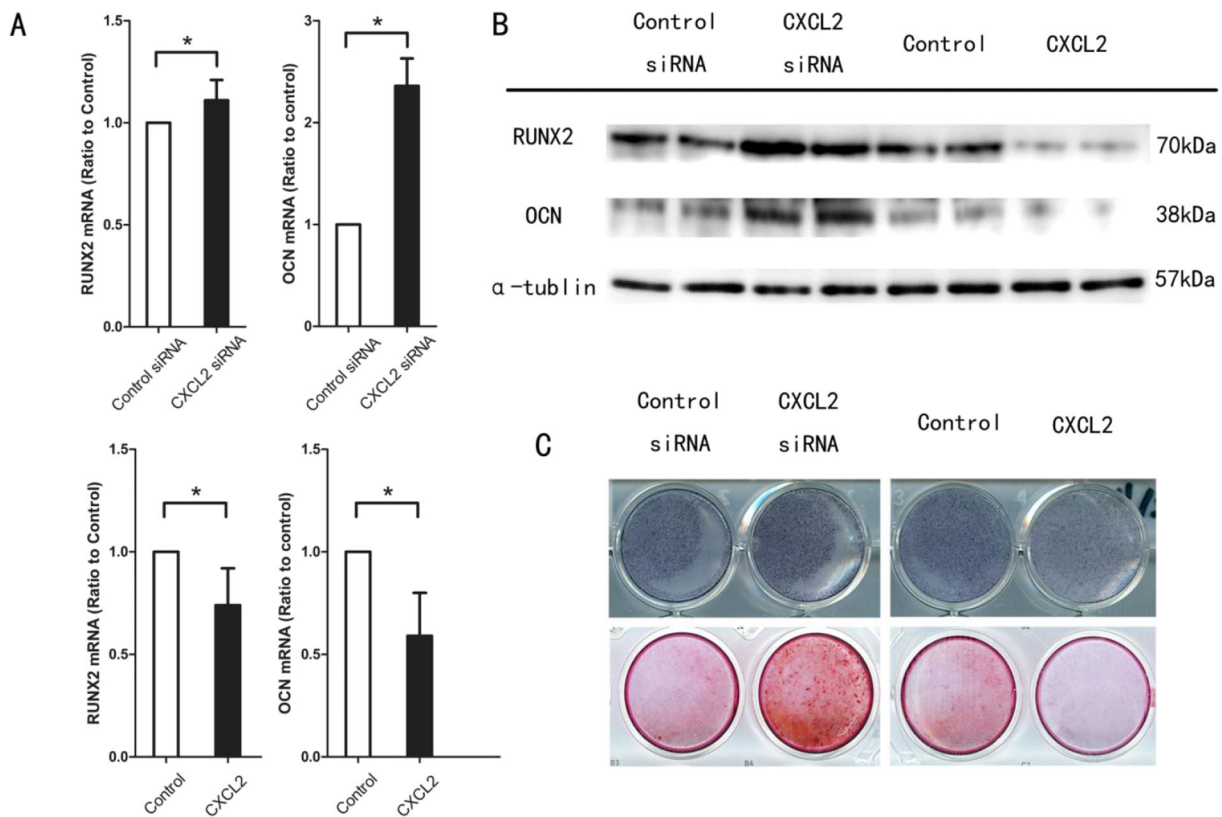
Fig. 5. qPCR, western blotting and osteogenic staining indicate that CXCL2 suppresses differentiation of MC3T3-E1 cells *in vitro*. (A) Quantification of *Runx2* and *Ocn* mRNA expression in MC3T3-E1 cells using qPCR analysis. Top: Cells transfected with negative control siRNA (control siRNA) or siRNA targeting *Cxcl2* (CXCL2 siRNA) to downregulate expression of *Cxcl2*). Bottom: Cells transfected with pCMV-Flag-NC (Control) or pCMV-Flag-CXCL2 (CXCL2) to upregulate expression of *Cxcl2*. Cells were isolated 24 h after transfection. *n*=6 per group. (B) Western blotting of RUNX2 and OCN in MC3T3-E1 cells transfected with negative control siRNA (control siRNA), siRNA targeting Cxcl2 (CXCL2 siRNA), pCMV-Flag-NC (Control) or pCMV-Flag-CXCL2 (CXCL2). Proteins were harvested 48 h after transfection. (C) ALP staining (top) and ARS (bottom) of transfected MC3T3-E1 cells 7 and 21 days after induction of osteogenic differentiation. *$P<0.05$.
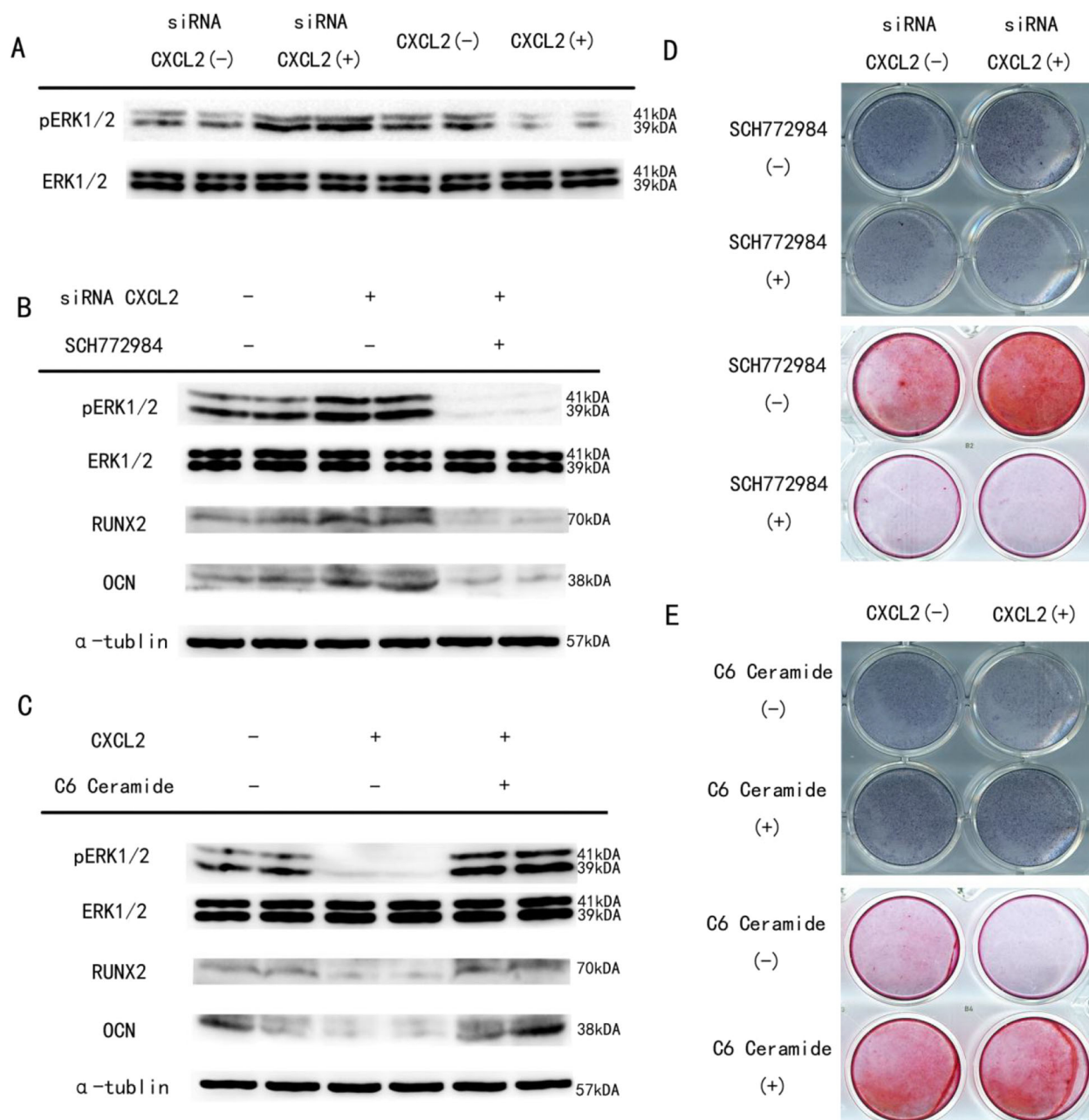
Fig. 6. Western blotting, ALP staining and ARS indicate that CXCL2 inhibits ERK1/2 signaling upstream of RUNX2 in MC3T3-E1 cells *in vitro*. (A) For western blot analysis of phosphorylated ERK1/2 (pERK1/2), MC3T3-E1 cells were treated with siRNA NC [siRNA CXCL2 (−)] or siRNA CXCL2 [siRNA CXCL2 (+)], or transfected with pCMV-Flag-NC [CXCL2 (−)] or pCMV-Flag-CXCL2 [CXCL(+)]. (B) MC3T3-E1 cells were treated with siRNA CXCL2 (+) or siRNA NC (−) and co-treated with SCH7729984 (+) or not (−). RUNX2, OCN, and pERK1/2 were analyzed by western blotting. (C) MC3T3-E1 cells were transfected with pCMV-Flag-CXCL2 (+) or pCMV-Flag-NC (−) and treated (+) or not with C6 ceramide (−). RUNX2, OCN and pERK1/2 were analyzed by western blotting. (D) ALP staining (top) on day 7 and ARS (bottom) on day 21 of MC3T3-E1 cells treated with siRNA CXCL2, cultured in inducing medium and treated or not with SCH7729984. (E) ALP staining (top) on day7 and ARS (bottom) on day 21 of MC3T3-E1 cells transfected with pCMV-Flag-CXCL2, cultured in inducing medium and treated or not with C6 ceramide.

transfected with a pCMV vector expressing a negative-control plasmid (pCMV-Flag-NC). Transfection efficiency was measured using real-time qPCR and microarray analysis. In some experiments, we also use primary osteoblast cultures of suckling mice (Fig. S1). The siRNAs and plasmids were purchased from GenePharma, Shanghai, China. Negative control siRNA sequences were as follows (5′-3′), Forward: UUCUCCGAACGUGUCAC-GUTT, Reverse: ACGUGACACGUUCGGAGAATT. siRNA targeting *Cxcl2* (siRNA CXCL2) were: Forward: GGGUUGACUUCAAGAACAUTT, Reverse: AUGUUCUUGAAGU-CAACCCTT.

Ki-67 and CCK8 proliferation assay

We performed immunofluorescence staining for the proliferation marker protein Ki-67 to detect proliferation in transfected MC3T3-E1 cells. Primary rabbit antiKi-67antibody specific to mouse (Abcam, #Ab16667, 1:500) was applied. The CCK8 kit (KeyGEN) was used following the manufacturer's instructions to assess cell proliferation. Transfected MC3T3-E1 cells were seeded into 96-well plates at 100 µl per well (3000 cells per well). Then, we examined proliferation of each group, i.e. cells transfected with control siRNA, CXCL2 siRNA, Control-expressing plasmid and CXCL2-

expressing plasmid at 12 h, 24 h, 36 h, and 48 h following seeding. The OD_{450} values were measured with an ultraviolet spectrophometer (NanoVue Plus, GE Healthcare).

Flow cytometry assay

Apoptosis of transfected MC3T3-E1 cells was analyzed by flow cytometry using a flow cytometry kit (BD, #556547). Cells were harvested 48 h after transfection and stained with annexin V conjugated to FITC and PI according to the manufacturer's instructions. The rate of apoptosis was evaluated using flow cytometry (Canto, BD Biosciences). All experiments were repeated three times.

RNA isolation and quantitative real-time PCR analysis

Total RNA from treated cells was extracted using Trizol Reagent (Life Technologies, #15596-018), following the manufacturer's protocol. The reverse transcriptase reaction was performed using PrimeScript reverse transcriptase (TaKaRa, #2680B). The cDNA was used for real-time PCR using TB Green Premix Ex Taq (TaKaRa, #RR420A) on a real-time PCR system (LightCycler96, Roche, Switzerland). For quantitative results, expression of each RNA is shown as the fold-change using the double delta Ct ($2^{-\Delta\Delta CT}$) analysis. The sequences of primer pairs are presented as follows (5′–3′): GAPDH, Forward: AGGTCGGTGTGAACGGATTTG, Reverse: TGTAGACCATGTAGTTGAGGTCA; CXCL2, Forward: TGCCGGCTCCTCAGTGCT, Reverse: GCCTTGCCTTTGTTCAGTATCTTTTG; RUNX2, Forward: GACTGTGGTTACCGTCATGGC, Reverse: ACTTGGTTTTTCATAACAGCGGA; OCN, Forward: AAGCCTTCATGTCCAAGCAGG, Reverse: TTTGTA- GGCGGTCTTCAAGCC.

Western blotting

Treated cells were lysed with 2% SDS, 2 M urea, 10% glycerol, 10 mM Tris-HCl pH 6.8, 10 mM dithiothreitol and 1 mM phenylmethylsulfonyl fluoride. Lysates were centrifuged and supernatants were separated by SDS-polyacrylamide gel electrophoresis and transferred onto polyvinylidene difluoride (PVDF) membranes (Merck Millipore Ltd). The PVDF membranes were then blocked at room temperature for 1 h and incubated overnight at 4°C with monoclonal antibodies against the following proteins: α-tublin (ABclonal, AC012, 1:5000), OCN (Santa Cruz, SC23790, 1:1000), RUNX2 (ABclonal, A2851, 1:1000), CXCL2 (R&D, AF-452-NA, 1:1000), ERK1 and ERK2 (HuaBio, ET1601-29, 1:1000), and phosphorylated (p)ERK1/2 (HuaBio, RT1206, 1:1000). After three washes in Tris-buffered saline and Tween 20 (TBST) for 5 min each, membranes were incubated with the corresponding secondary antibodies (HRP Donkey Anti-Goat IgG #AS031, HRP Donkey Anti-Mouse IgG #AS033, HRP Donkey Anti-Rabbit IgG #AS038, all ABclonal;) 1:1000) at room temperature for 1 h. Bands were analyzed using an enhanced chemiluminescence system.

Alkaline phosphatase activity and mineralization assay

Transfected MC3T3-E1 cells were cultured in inducing medium, and staining with alkaline phosphatase (ALP) and Alizarin Red staining (ARS) was performed to evaluate the ability of treated cells to differentiate into osteocytes, i.e. their level of osteogenic differentiation. MC3T3-E1 cells were cultured in 12-well plates. After transfection, the medium was replaced with inducing medium. In some experiments, transfected MC3T3-E1 cells were co-treated with the ERK1/2 inhibitor SCH772984 (0.6 nmol per well) or the ERK1/2 activator C6 ceramide (40 μmol per well). C6 ceramide nanoliposomes were prepared as described in an earlier study (Ryland et al., 2013). ALP staining was performed 7 days after induction of osteogenic differentiation, and ARS was performed 21 days after induction. Analyses were carried out according to the manufacturer's instructions of the Modified calcium-cobalt method ALP staining kit (Beyotime, catalog: P0321) and the standard techniques of the ARS kit (Solarbio).

Statistics

All data are presented as the mean±s.d. Curve analysis was carried out using Prism (GraphPad).Data in each group were analyzed using the unpaired, two-tailed Student's t-test or the Pearson correlation analysis. The level of significance was set at $P<0.05$.

References

Abrahamsen, B., Skjødt, M. K. and Vestergaard, P. (2018). Hip fracture rates and time trends in use of anti-osteoporosis medications in Denmark for the period 2005 to 2015: missed opportunities in fracture prevention. *Bone* **120**, 476-481. doi:10.1016/j.bone.2018.12.016

Ansel, K. M. and Cyster, J. G. (2001). Chemokines in lymphopoiesis and lymphoid organ development. *Curr. Opin. Immunol.* **13**, 172-179. doi:10.1016/S0952-7915(00)00201-6

Arron, J. R. and Choi, Y. (2000). Bone versus immune system. *Nature* **408**, 535-536. doi:10.1038/35046196

Baggiolini, M. (1998). Chemokines and leukocyte traffic. *Nature* **392**, 565-568. doi:10.1038/33340

Baird, A. M., Gerstein, R. M. and Berg, L. J. (1999). The role of cytokine receptor signaling in lymphocyte development. *Curr. Opin. Immunol.* **11**, 157-166. doi:10.1016/S0952-7915(99)80027-2

Boutros, T., Chevet, E. and Metrakos, P. (2008). Mitogen-activated protein (MAP) kinase/MAP kinase phosphatase regulation: roles in cell growth, death, and cancer. *Pharmacol. Rev.* **60**, 261-310. doi:10.1124/pr.107.00106

Cargnello, M. and Roux, P. P. (2011). Activation and function of the MAPKs and their substrates, the MAPK-activated protein kinases. *Microbiol. Mol. Biol. Rev.* **75**, 50-83. doi:10.1128/MMBR.00031-10

Clarke, C., Kuboki, S., Sakai, N., Kasten, K. R., Tevar, A. D., Schuster, R., Blanchard, J., Caldwell, C. C., Edwards, M. J. and Lentsch, A. B. (2011). CXC chemokine receptor-1 is expressed by hepatocytes and regulates liver recovery after hepatic ischemia/reperfusion injury. *Hepatology* **53**, 261-271. doi:10.1002/hep.24028

D'Amelio, P., Grimaldi, A., Di Bella, S., Brianza, S. Z. M., Cristofaro, M. A., Tamone, C., Giribaldi, G., Ulliers, D., Pescarmona, G. P. and Isaia, G. (2008). Estrogen deficiency increases osteoclastogenesis up-regulating T cells activity: a key mechanism in osteoporosis. *Bone* **43**, 92-100. doi:10.1016/j.bone.2008.02.017

Eswarakumar, V., Lax, I. and Schlessinger, J. (2005). Cellular signaling by fibroblast growth factor receptors. *Cytokine Growth F. R.* **16**, 139-149. doi:10.1016/j.cytogfr.2005.01.001

Fagerberg, L., Hallström, B. M., Oksvold, P., Kampf, C., Djureinovic, D., Odeberg, J., Habuka, M., Tahmasebpoor, S., Danielsson, A., Edlund, K. et al. (2014). Analysis of the human tissue-specific expression by genome-wide integration of transcriptomics and antibody-based proteomics. *Mol. Cell. Proteomics* **13**, 397-406. doi:10.1074/mcp.M113.035600

Franceschi, R. T., Ge, C., Xiao, G., Roca, H. and Jiang, D. (2007). Transcriptional regulation of osteoblasts. *Ann. N. Y. Acad. Sci.* **1116**, 196-207. doi:10.1196/annals.1402.081

Glaser, D. L. and Kaplan, F. S. (1997). Osteoporosis, definition and clinical presentation. *Spine* **58**, 12s-16s. doi:10.1097/00007632-199712151-00003

Greenblatt, M. B., Shim, J.-H. and Glimcher, L. H. (2013). Mitogen-activated protein kinase pathways in osteoblasts. *Annu. Rev. Cell Dev. Biol.* **29**, 63-79. doi:10.1146/annurev-cellbio-101512-122347

Ha, Y.-C. (2016). Epidemiology of osteoporosis in Korea. *J. Korean Med. Assoc.* **59**, 836-841. doi:10.5124/jkma.2016.59.11.836

Ha, J., Choi, H.-S., Lee, Y., Kwon, H.-J., Song, Y. W. and Kim, H.-H. (2010). CXC chemokine ligand 2 induced by receptor activator of NF-kappa B ligand enhances osteoclastogenesis. *J. Immunol.* **184**, 4717-4724. doi:10.4049/jimmunol.0902444

Hu, B. and Colletti, L. M. (2010). CXC receptor-2 knockout genotype increases X-linked inhibitor of apoptosis protein and protects mice from acetaminophen hepatotoxicity. *Hepatology* **52**, 691-702. doi:10.1002/hep.23715

Huang, B., Wang, Y., Wang, W., Chen, J., Lai, P., Liu, Z., Yan, B., Xu, S., Zhang, Z., Zeng, C. et al. (2015). mTORC1 prevents preosteoblast differentiation

through the Notch signaling pathway. *PLoS Genet.* **11**, e1005426. doi:10.1371/journal.pgen.1005426

Huang, B., Wang, W., Li, Q., Wang, Z., Yan, B., Zhang, Z., Wang, L., Huang, M., Jia, C., Lu, J. et al. (2016). Osteoblasts secrete Cxcl9 to regulate angiogenesis in bone. *Nat. Commun.* **7**, 13885. doi:10.1038/ncomms13885

Ijichi, H., Chytil, A., Gorska, A. E., Aakre, M. E., Bierie, B., Tada, M., Mohri, D., Miyabayashi, K., Asaoka, Y., Maeda, S. et al. (2011). Inhibiting Cxcr2 disrupts tumor-stromal interactions and improves survival in a mouse model of pancreatic ductal adenocarcinoma. *J. Clin. Invest.* **121**, 4106-4117. doi:10.1172/JCI42754

Kageyama, S., Nakamura, K., Fujii, T., Ke, B., Sosa, R. A., Reed, E. F., Datta, N., Zarrinpar, A., Busuttil, R. W. and Kupiec-Weglinski, J. W. (2018). Recombinant relaxin protects liver transplants from ischemia damage by hepatocyte glucocorticoid receptor: from bench-to-bedside. *Hepatology* **68**, 258-273. doi:10.1002/hep.29787

Kanis, J. A., Oden, A., Johnell, O., Jonsson, B., De Laet, C. and Dawson, A. (2001). The burden of osteoporotic fractures: a method for setting intervention thresholds. *Osteoporos. Int.* **12**, 417-427. doi:10.1007/s001980170112

Lasagni, L., Grepin, R., Mazzinghi, B., Lazzeri, E., Meini, C., Sagrinati, C., Liotta, F., Frosali, F., Ronconi, E., Alain-Courtois, N. et al. (2007). Alain-Courtois N PF-4/CXCL4 and CXCL4L1 exhibit distinct subcellular localization and a differentially regulated mechanism of secretion. *Blood* **109**, 4127-4134. doi:10.1182/blood-2006-10-052035

Liu, Y., Shepherd, E. G. and Nelin, L. D. (2007). MAPK phosphatases–regulating the immune response. *Nat. Rev. Immunol.* **7**, 202-212. doi:10.1038/nri2035

Lizneva, D., Yuen, T., Sun, L., Kim, S.-M., Atabiekov, I., Munshi, L. B., Epstein, S., New, M. and Zaidi, M. (2018). Emerging concepts in the epidemiology, pathophysiology, and clinical care of osteoporosis across the menopausal transition. *Matrix Biol.* **71-72**, 70-81. doi:10.1016/j.matbio.2018.05.001

Long, F. (2012). Building strong bones: molecular regulation of the osteoblast lineage. *Nat. Rev. Mol. Cell Biol.* **13**, 27-38. doi:10.1038/nrm3254

Maeda, A., Bandow, K., Kusuyama, J., Kakimoto, K., Ohnishi, T., Miyawaki, S. and Matsuguchi, T. (2015). Induction of CXCL2 and CCL2 by pressure force requires IL-1β-MyD88 axis in osteoblasts. *Bone* **74**, 76-82. doi:10.1016/j.bone.2015.01.007

Manolagas, S. C. (2000). Birth and death of bone cells: basic regulatory mechanisms and implications for the pathogenesis and treatment of osteoporosis. *Endocr. Rev.* **21**, 115-137. doi:10.1210/er.21.2.115

Marini, F., Cianferotti, L. and Brandi, M. L. (2016). Epigenetic mechanisms in bone biology and osteoporosis: can they drive therapeutic choices? *Int. J. Mol. Sci.* **17**, 1329. doi:10.3390/ijms17081329

Mcnamara, L. M. (2010). Perspective on post-menopausal osteoporosis: establishing an interdisciplinary understanding of the sequence of events from the molecular level to whole bone fractures. *J. R Soc. Interface* **44**, 353-372. doi:10.1098/rsif.2009.0282

Murakami, J., Ishii, M., Suehiro, F., Ishihata, K., Nakamura, N. and Nishimura, M. (2017). Vascular endothelial growth factor-C induces osteogenic differentiation of human mesenchymalstem cells through the ERK and RUNX2 pathway. *Biochem. Biophys. Res. Commun.* **484**, 710-718. doi:10.1016/j.bbrc.2017.02.001

National Clinical Guideline (2012). *Osteoporosis: Fragility Fracture Risk: Osteoporosis: Assessing the Risk of Fragility Fracture. Royal College of Physicians (UK) National Clinical Guideline Centre*. London, UK: National Institute for Health and Clinical Excellence: Guidance.

Ornitz, D.M and Marie, P.J. (2002). FGF signaling pathways in endochondral and intramembranous bone development and human genetic disease. *Gene. Dev.* **16**, 1446-1465. doi:10.1101/gad.990702

Qin, C.-C., Liu, Y.-N., Hu, Y., Yang, Y. and Chen, Z. (2017). Macrophage inflammatory protein-2 as mediator of inflammation in acute liver injury. *World J. Gastroenterol.* **23**, 3043-3052. doi:10.3748/wjg.v23.i17.3043

Rittner, H. L., Labuz, D., Richter, J. F., Brack, A., Schäfer, M., Stein, C. and Mousa, S. A. (2007). CXCR1/2 ligands induce p38 MAPK-dependent translocation and release of opioid peptides from primary granules in vitro and in vivo. *Brain Behav. Immun.* **21**, 1021-1032. doi:10.1016/j.bbi.2007.05.002

Rollins, R. J. (1997). Chemokines. *Blood* **90**, 909-928.

Ryland, L. K., Doshi, U. A., Shanmugavelandy, S. S., Fox, T. E., Aliaga, C., Broeg, K., Young, M., Khan, O., Haakenson, J. K., Jarbadan, N. R. et al. (2013). C6-ceramide nanoliposomes target the Warburg effect in chronic lymphocytic leukemia. *PLoS ONE* **8**, e84648. doi:10.1371/journal.pone.0084648

Scala, S. (2015). Molecular pathways: targeting the CXCR4-CXCL12 axis– untapped potential in the tumor microenvironment. *Clin. Cancer Res.* **21**, 4278-4285. doi:10.1158/1078-0432.CCR-14-0914

Strieter, R. M., Gomperts, B. N. and Keane, M. P. (2007). The role of CXC chemokines in pulmonary fibrosis. *J. Clin. Invest.* **117**, 549-556. doi:10.1172/JCI30562

Trošt, Z., Trebše, R., Preželj, J., Komadina, R., Logar, D. B. and Marc, J. (2010). A microarray based identification of osteoporosis-related genes in primary culture of human osteoblasts. *Bone* **46**, 72-80. doi:10.1016/j.bone.2009.09.015

Valerio, M. S., Herbert, B. A., Basilakos, D. S., Browne, C., Yu, H. and Kirkwood, K. L. (2015). Critical role of MKP-1 in lipopolysaccharide-induced osteoclast formation through CXCL1 and CXCL2. *Cytokine* **71**, 71-80. doi:10.1016/j.cyto.2014.08.007

Vandercappellen, J., Van Damme, J. and Struyf, S. (2008). The role of CXC chemokines and their receptors in cancer. *Cancer Lett.* **267**, 226-244. doi:10.1016/j.canlet.2008.04.050

Van Sweringen, H. L., Sakai, N., Tevar, A. D., Burns, J. M., Edwards, M. J. and Lentsch, A. B. (2011). CXC chemokine signaling in the liver: impact on repair and regeneration. *Hepatology* **54**, 1445-1453. doi:10.1002/hep.24457

Verbeke, H., Struyf, S., Laureys, G. and Van Damme, J. (2011). The expression and role of CXC chemokines in colorectal cancer. *Cytokine Growth Factor. Rev.* **5-6**, 345-358. doi:10.1016/j.cytogfr.2011.09.002

Wasmuth, H. E., Lammert, F., Zaldivar, M. M., Weiskirchen, R., Hellerbrand, C., Scholten, D., Berres, M.-L., Zimmermann, H., Streetz, K. L., Tacke, F. et al. (2009). Antifibrotic effects of CXCL9 and its receptor CXCR3 in livers of mice and humans. *Gastroenterology* **137**, 309-319. doi:10.1053/j.gastro.2009.03.053

Wolpe, S. D., Sherry, B., Juers, D., Davatelis, G., Yurt, R. W. and Cerami, A. (1989). Identification and characterization of macrophage inflammatory protein 2. *Proc. Natl. Acad. Sci. USA* **86**, 612-616. doi:10.1073/pnas.86.2.612

Wong, S. Y., Tan, M. G. K., Banks, W. A., Wong, W. S. F., Wong, P. T.-H. and Lai, M. K. P. (2016). Andrographolide attenuates LPS-stimulated up-regulation of C-C and C-X-C motif chemokines in rodent cortex and primary astrocytes. *J. Neuroinflammation* **13**, 34. doi:10.1186/s12974-016-0498-6